Defining the Region of Troponin-I that Binds to Troponin-C†

Ryan T. McKay, Brian P. Tripet, Joyce R. Pearlstone, Lawrence B. Smillie, and Brian D. Sykes*

MRC Group in Protein Structure and Function, Department of Biochemistry, 474 Medical Sciences Building, University of Alberta, Canada T6G 2H7

Received December 17, 1998; Revised Manuscript Received February 23, 1999

ABSTRACT: The kinetics and energetics of the binding of three troponin-I peptides, corresponding to regions 96−131 (TnI_{96-131}), 96−139 (TnI_{96-139}), and 96−148 (TnI_{96-148}), to skeletal chicken troponin-C were investigated using multinuclear, multidimensional NMR spectroscopy. The kinetic off-rate and dissociation constants for TnI_{96-131} (400 s^{-1}, 32 μM), TnI_{96-139} (65 s^{-1}, <1 μM), and TnI_{96-148} (45 s^{-1}, <1 μM) binding to TnC were determined from simulation and analysis of the behavior of ^1H,^{15}N-heteronuclear single quantum correlation NMR spectra taken during titrations of TnC with these peptides. Two-dimensional ^{15}N-edited TOCSY and NOESY spectroscopy were used to identify 11 C-terminal residues from the ^{15}N-labeled TnI_{96-148} that were unperturbed by TnC binding. TnI_{96-139} labeled with ^{13}C at four positions (Leu^{102}, Leu^{111}, Met ^{121}, and Met^{134}) was complexed with TnC and revealed single bound species for Leu^{102} and Leu^{111} but multiple bound species for Met^{121} and Met^{134}. These results indicate that residues 97−136 (and 96 or 137) of TnI are involved in binding to the two domains of troponin-C under calcium saturating conditions, and that the interaction with the regulatory domain is complex. Implications of these results in the context of various models of muscle regulation are discussed.

The transient release of calcium in a muscle cell in response to a neural signal results in a cascade of changing protein·protein interactions and eventually muscle contraction (for review, see refs *1*−*4*). The sliding of the thick and thin filaments past one another constitutes the actual physical mechanism of contraction produced as a result of the hydrolysis of ATP by myosin. The regulatory target for calcium in skeletal muscle cells is the troponin complex consisting of troponin-C (TnC),[1] troponin-I, and troponin-T. TnC is the calcium-binding component and is the only member of the complex presently resolved at an atomic level. TnI inhibits the ability of myosin to hydrolyze ATP, thus preventing muscle contraction. Troponin-T anchors the troponin complex to actin/tropomyosin, interacts with TnC directly, and is involved in the activation of contraction in the presence of calcium (see ref *5* and references therein). Once calcium is released in the cell, the three-dimensional structure of TnC and subsequent protein·protein interactions are altered. Specifically, TnC in the presence of calcium interacts with TnI more strongly and allows muscle contraction to occur (see refs *1*, *2*, *6*, *7*, and references therein). However, the exact mechanism of how TnI inhibits contraction in the absence of calcium, and conversely participates in the activation of the actomyosin complex in the presence of calcium, is not presently understood.

TnC is an 18 kDa protein of 162 amino acids comprising 2 separate domains (N- and C-domains each ∼80 amino acids) covalently attached by a flexible "helical" linker (residues ∼80−95). Both the C- and N-terminal domains are predominantly α-helical with each individual domain containing two EF hand calcium-binding sites that interact through a short bisecting β-sheet. The calcium-binding sites are labeled sequentially I−IV on the basis of their respective positions in the primary amino acid sequence of the protein. The C-terminal sites have a higher affinity for Ca^{2+} than the N-terminal sites, and the C-terminal sites also have affinity for Mg^{2+} while the N-terminal sites are calcium-specific. Sites I and II have calcium affinities ($\sim 7 \times 10^4$ and 5×10^5 M^{-1} for K_a, respectively) in the range of the transient Ca^{2+} signal (*8*). It has not been determined if the C-terminal sites are bound with Mg^{2+} at all times, or if the Ca^{2+} signal is of sufficient duration to displace Mg^{2+} in the contractile state.

There is presently no high-resolution structure for TnC with Mg^{2+} bound in sites III and IV, but there are several crystal structures of skeletal TnC with calcium present in the C-domain, and absent from (*9*, *10*) or present in the N-domain (*11*−*13*). NMR solution structures include that

† This work was supported by the Medical Research Council Group in Protein Structure and Function, a Faculty of Medicine 75th Anniversary Studentship (R.T.M.), and by two Alberta Heritage Foundation for Medical Research Studentships (R.T.M. and B.P.T.).

* To whom correspondence should be addressed. Tel: (403) 492-5460. Fax: (403) 492-0886. E-mail: brian.sykes@ualberta.ca and rtm@polaris.biochem.ualberta.ca.

[1] Abbreviations: TnC, whole skeletal chicken troponin-C; TnI, skeletal troponin-I; TnI_x, synthetic skeletal troponin-I peptide containing residues designated by the subscript value "x"; N-TnC, N-domain of skeletal chicken troponin-C; TnC·TnI_{96-131}, [U-^{15}N,^{13}C]TnC·TnI_{96-131}; TnC·TnI_{96-139}, [U-^{15}N, ^{13}C-Ala]TnC·TnI_{96-139}; TnC·TnI_{96-148}, [U-^{15}N,^{13}C-Ala]TnC·TnI_{96-148}; ^{15}N-TnI_{96-148}, [U-^{15}N]TnI_{96-148}; ^{13}C-TnI_{96-139}, [U-^{13}C-(100%)Leu^{102},-(50%)Leu^{111}, $^{13}CH_3$-(100%)Met^{121},-(50%)Met^{134}]TnI_{96-139}; ^{15}N-TnI_{96-148}·TnC, [U-^2H]TnC·[U-^{15}N]TnI_{96-148}; ^{13}C-TnI_{96-139}·TnC, [U-^2H,^{15}N]TnC·[U-^{13}C-(100%)Leu^{102},-(50%)Leu^{111}, $^{13}CH_3$-(100%)-Met^{121},-(50%)Met^{134}]TnI_{96-139}; HSQC, 2D-^{15}N-edited heteronuclear single quantum correlation NMR spectroscopy; ^{13}C-HSQC, 2D-^{13}C-edited heteronuclear single quantum correlation NMR spectroscopy; $\Delta\delta$, change ($\sqrt{\Delta\delta^2_{1H}+\Delta\delta^2_{15N}}$) in chemical shift (Hz) of a backbone amide cross-peak as monitored by HSQC spectroscopy; $\Delta\delta_{total}$, the $\sum\Delta\delta^i$ over all monitored residues at each point of the titration; $\Delta G^{\ddagger}_{off}$, activation energy of the reverse reaction.

10.1021/bi9829736 CCC: $18.00
Published on Web 04/03/1999

of apo and Ca^{2+}-saturated N-TnC (*14*), Ca^{2+}-saturated E41A N-TnC (*15*), Ca^{2+}-saturated TnC (*16*), both apo and Ca^{2+}-saturated cardiac N-TnC (*17*), cardiac TnC (*18*), and Ca^{2+}-saturated N-TnC while bound to TnI_{96-148} (*19*) (see ref *20* for an overall review and comparison of the solution and X-ray troponin-C structures). The structures have revealed important information regarding the mechanism of both cardiac and skeletal muscle regulation. In the skeletal system the binding of calcium in the low-affinity sites causes the movement of the B and C helices away from the N, A, and D helices (*14*), exposing a hydrophobic pocket that has been shown to bind TnI (*19*, *21*). Interestingly, this large structural change is not observed in cardiac TnC upon binding calcium. Recently, the X-ray crystal structure of $2Ca^{2+}$ (sites III and IV occupied) skeletal TnC while bound with a TnI peptide (residues 1−47) was reported (*22*, *23*).

Calmodulin and the myosin light chains are very highly homologous, multiple EF hand motif-containing, dumbbell-shaped, calcium-binding proteins that have also been resolved at an atomic level (see ref *24* for review). The structures of CaM, bound to skeletal or smooth muscle myosin light chain kinase peptides (*25*, *26*), a brain CaM-dependent protein kinase IIα peptide (*27*), and the regulatory and essential light chains of myosin bound to a portion of the heavy chain (*28*), have revealed different manners in which the N- and C-terminal domains of calcium regulatory proteins interact with protein targets (see ref *29* and references therein). These structures and other experiments involving various target peptides suggest that calcium-binding proteins may be able to bind using both domains in an extended structure, or both domains in a collapsed orientation to grasp target peptides.

Despite the structural information presently available for TnC and the homologous CaM and myosin systems, there is relatively little known about TnI either in isolation or in complex with TnC and/or TnT. We do not know exactly which residues of TnI interact with TnC under conditions normally associated with the contractile or relaxed states, nor do we fully understand the mechanism or nature of the interaction. However, on the basis of a variety of experimental approaches, evidence for an antiparallel arrangement of TnC and TnI molecules (*2*) in an extended, partially extended, or compact structure has been deduced (*23*, *30*−*32*) and a number of interaction sites identified (see below). Studies have included cross-linking (*33*−*38*), low-angle X-ray diffraction of TnC·TnI (*30*, *39*, *40*), ATPase assays of various combinations of both intact proteins and their fragments in the presence or absence of Ca^{2+} (*41*−*43*), and binding studies of intact TnC, N-TnC, C-TnC with TnI, and its peptide fragments (i.e., proteolytic, synthetic, or recombinant) by gel electrophoresis, fluorescence, and NMR measurements (*19*, *21*, *44*−*48*).

These studies have identified two regions (1−21 and 96−148) of the TnI polypeptide chain important in Ca^{2+}-dependent interaction with TnC. TnI residues 1−40 appeared to bind exclusively to the C-domain of TnC with a low dissociation constant ($K_d < 10^{-7}$ M) in the presence of Ca^{2+} (*49*). This affinity is weakened when Ca^{2+} is replaced by Mg^{2+} (*50*). These observations are consistent with other studies (*5*, *41*) using longer fragments of TnI (i.e., residues 1−98 and 1−116). The recently reported 2.3 Å X-ray structure of 2 Ca^{2+} TnC in complex with TnI_{1-47} shows a "compact" TnC structure with multiple proposed contacts from both N- and C-terminal domains of TnC to the peptide. On the basis of their structure and other data they have proposed a model. It is presently unclear how representative this model is of the complex of calcium-saturated TnC with intact TnI (or fragments derived from its central and/or C-terminal regions).

The latter segments of TnI are the major focus of this present investigation. Residues 96−116 have long been recognized as containing the major inhibitory activity of TnI (i.e., residues 104−115 known as the inhibitory region) (*7*, *51*, *52*). Interaction of the inhibitory region with TnC has been localized to the C-domain and possibly the linker (i.e., the D/E helix in X-ray structure) between the N- and C-domains. More recently a section of TnI (i.e., residues ∼115−148) has been recognized as contributing significantly to inhibition and to Ca^{2+} sensitivity of the ATPase activity in the reconstituted troponin·tropomyosin actomyosin system (*41*, *43*). In a comparison of binding affinities of TnI_{96-116} and TnI_{96-148} to calcium-saturated TnC and its isolated N- and C-domains, the binding to the N-domain of TnC was significantly increased with the extended fragment, and a 3-fold repeated sequence motif has been reported, specifically involving TnI residues 101−114, 121−132, and 135−146 (*47*). By using a variety of synthetic peptides encompassing residues 96−148, Tripet et al. (*32*) have demonstrated the importance of lysine residues 141, 144, and 145 for full inhibitory activity (i.e., binding to tropomyosin/actin) and the importance of the 116−126 region in binding to TnC. Two models have been suggested. The first contains a "switching mechanism" that is dependent on the presence of calcium in the N-domain of TnC (refs *30*, *32*, and references therein), while the second model has the N-terminal TnI residues (∼1−47) specifically involved in calcium-independent binding to the hydrophobic pocket of C-TnC (*22*, *23*). There is presently no definitive experiment to decide between either model.

In an attempt to provide more detailed information on the interface between the two components of the TnC·TnI complex, this laboratory has applied multinuclear, multidimensional NMR spectroscopy to the interaction of TnC with TnI peptides, specifically in the 96−148 region. Studies to date have provided dissociation constants for $TnI_{115-131}$ and TnI_{96-148} in complex with calcium-saturated N-TnC and identified residues perturbed by binding of these peptides (*19*, *21*). The data confirm that TnI peptide binding involves interactions with residues in the hydrophobic pocket of N-TnC. The present report extends these studies to a comparison of the binding kinetics and energetics of TnI_{96-131}, TnI_{96-139}, and TnI_{96-148} to calcium-saturated, intact TnC. In addition to providing the dissociation and kinetic off-rates for these peptides, the NMR spectral data of the labeled TnI peptide show that residues 97−136 are the residues within the 96−148 region primarily involved in binding to calcium-saturated TnC. Also, a specifically ^{13}C-labeled TnI_{96-139} peptide when complexed to TnC indicates that the N-terminal region of the TnI peptide appears to bind in a single orientation (presumably to the C-domain of TnC), while the C-terminal region of TnI assumes multiple bound conformations.

EXPERIMENTAL PROCEDURES

Proteins and Peptides. The cloning, expression, and purification of [U-^{15}N,^{13}C-Ala] TnC, [U-^{15}N,^{13}C] TnC, and [U-^{2}H (88%)] TnC were performed as described previously (*21*, *53*). Synthetic N$^{\alpha}$-acetyl peptides corresponding to rabbit skeletal troponin-I regions 96−131, 96−139, and 96−148 were prepared as described by Tripet et al. (*32*). Synthetic N$^{\alpha}$-acetyl TnI$_{96-139}$ incorporating [U-^{13}C]-L-leucine (residues 102 and 111) and [^{13}CH$_3$]-L-methionine (residues 121 and 134) was prepared as the other peptides except for manual synthesis runs at each labeled position. Leucine at position 102 was 100% labeled while the synthesis of position 111 was performed with only 50% labeled leucine, as was the case for methionine positions 121 (100%) and 134 (50%), respectively. The uniformly ^{15}N-labeled TnI$_{96-148}$ peptide was produced from the cloning and transformation of pAED4·TnI$_{96-148}$ into *Escherichia coli* strain BL21·DE3·pLysS (Novagen) for inducible protein expression with 0.4 mM IPTG. The purification of expressed TnI$_{96-148}$ from an extract of dried acetone powder cell pellet, on a CM-cellulose column at pH 7.5, has been described previously (*47*). To produce uniformly ^{15}N-labeled protein, we initially grew cells in ZB medium (*54*) supplemented with ampicillin and chloramphenicol (both at 0.1 mg/mL) to $A_{600} \approx 0.7$. Ten milliliters of this culture was inoculated into each of four, 1 L volumes of M9 medium (*55*), in which NH_4Cl was replaced with 99.4% ^{15}N-enriched $(NH_4)_2SO_4$ (Isotec Inc.). The M9 minimal medium was supplemented with filter-sterilized solutions of minerals (final concentration of 2 mM $MgSO_4$, 1 μM $FeCl_3$, 25 μM $ZnSO_4$, and 0.1 mM $CaCl_2$), ampicillin, chloramphenicol, and vitamins (1 mg each of D-biotin, choline chloride, folic acid, niacimamide, D-pantothenic acid, and pyridoxine, 5 mg of thiamine, and 0.1 mg of riboflavin per liter). The concentration and primary sequence of proteins and peptides were confirmed by amino acid analysis done in quadruplicate, the correct mass verified by electrospray mass spectrometry, and the overall purity confirmed by reverse-phase HPLC.

NMR Sample Preparation. NMR samples were prepared for each of the [U-^{15}N,^{13}C]TnC·TnI$_{96-131}$, [U-^{15}N, ^{13}C-Ala]-TnC·TnI$_{96-139}$, [U-^{15}N,^{13}C-Ala]TnC·TnI$_{96-148}$, [U-^{2}H]TnC·[U-^{15}N]TnI$_{96-148}$, and [U-^{2}H,^{15}N]TnC·[U-^{13}C (100%) Leu^{102}, (50%) Leu^{111}, ^{13}CH$_3$ (100%) Met^{121}, (50%) Met^{134}]TnI$_{96-139}$ complexes. All titration samples started with 500 μL volumes. The [U-^{2}H]TnC·[U-^{15}N]TnI$_{96-148}$ complex sample had a volume of 500 μL with peptide and protein concentrations of 5×10^{-4} and 6×10^{-4} M, respectively. The ^{13}C-TnI$_{96-139}$·TnC complex sample had a volume of 500 μL with peptide and protein concentrations of 1.2 mM each. All NMR samples consisted of 90% H_2O, 10% D_2O, 10 mM deuterated imidazole, 100 mM KCl, 0.1 mM 2,2-dimethyl-2-silapentane-5-sulfonate as an internal reference standard, and slight amounts of HCl and/or NaOH as necessary to change the pH of the samples to 6.8 (uncorrected for isotope effects). Each sample contained 8 equiv of calcium per molecule of TnC (i.e., 2 mol per Ca^{2+}-binding site). Imidazole has been calibrated and was used as an internal pH reference standard (data not shown).

Titrations of TnC with TnI Peptides. Three separate titrations were performed. In each case TnC was titrated with the addition of a TnI peptide, and 2D-^{1}H,^{15}N-HSQC NMR spectra were taken at each point. In the first titration 5 μL of stock TnI$_{96-131}$ (5.1×10^{-8} mol/addition) were added to 500 μL of TnC (0.65 mM) achieving a final ratio of 1.54/1, peptide to TnC. The second titration involved adding 5 μL of stock TnI$_{96-139}$ (6.3×10^{-8} mol/addition) to 500 μL of TnC (0.85 mM) to a final ratio of 1.48/1, peptide to TnC. In the first two titrations the final addition of peptide was only 4 μL because 1 μL had been set aside for amino acid analysis. The third titration employing the TnI$_{96-148}$ peptide was found to have precipitation upon complex formation, and therefore amino acid analysis was performed before and after titration. Stock TnI$_{96-148}$ was added 10 times in 5 μL aliquots (2.25×10^{-8} mol/addition) to 500 μL of TnC (0.4 mM) to a final ratio of 1.1/1, peptide to protein.

NMR Spectroscopy and Assignment. Experiments were conducted on a Varian Unity-600 (titrations, TOCSY, and NOESY) or an Inova 500 (^{13}C-HSQC) spectrometer, and spectra were referenced according to Wishart et al. (*56*). The HSQC (*57*, *58*) spectra for the TnC·TnI$_{96-131}$, TnC·TnI$_{96-139}$, and TnC·TnI$_{96-148}$ titrations were acquired at 31 °C with sweep widths of 8000 Hz (all spectra acquired at 512 complex t_2 points) and 1650.2 Hz (128, 96, and 96 complex t_1 points for the first through third titrations, respectively) for the directly and indirectly detected dimensions, respectively, and with 24 transients/increment. The 2D-^{15}N-edited-TOCSYHSQC (*59*) spectra collected on the ^{15}N-TnI$_{96-148}$·TnC complex was acquired at 25 °C with 6500 Hz sweep widths in the indirectly (352 complex t_1 points) and directly (512 complex t_2 points) detected dimensions, respectively, and with 256 transients/increment. Both the 150 and 75 ms mixing time 2D-^{15}N-edited-NOESYHSQC (*59*) experiments were collected at 25 °C with 7000 Hz sweep widths in both the directly and indirectly detected dimensions. The 75 ms mixing time NOESYHSQC had 512 complex points in both dimensions with 80 transients/increment, while the 150 ms experiment had 256 t_1 complex points, 512 t_2 complex points, and 256 transients/increment. The ^{13}C-HSQCs for the ^{13}C-TnI$_{96-139}$ peptide and ^{13}C-TnI$_{96-139}$·TnC complex were done at 31 °C, and had 7000 Hz (2048 t_2 complex points) and 5500 Hz sweep widths (1536 t_2 complex points) for the directly detected dimension, respectively. Both ^{13}C-HSQCs were acquired with a sweep width of 2000 Hz (56 complex t_1 points) for the indirectly detected dimension, and mirror-image linear prediction was used to double the number of complex points. Carbon decoupling was not performed during the extended, directly detected acquisition period (293 ms) to prevent probe damage.

All directly and indirectly detected data sets were zero filled to twice the number of acquired (plus predicted when used) points, and spectra were apodized using a shifted sine bell before Fourier transformation. The acquisition time for HSQC experiments was approximately 4 h while ~1.5 days was required for each of the TOCSY and NOESY experiments. All experiments were processed and analyzed using the software packages NMRPipe and NMRDraw (*60*). Assignment of the TOCSY and NOESY experiments was performed as described previously (*61*, *62*).

Dissociation Constants. Two procedures were used to determine the equilibrium dissociation constants for the reaction of TnC with the TnI peptides. For TnI$_{96-131}$ the total chemical shift change of the well-resolved amide proton HSQC cross-peaks was monitored during the titration as a

function of added TnI_{96-131}. The changes were fit to both simple 1:1 binding

$$P + L \underset{k_{off}}{\overset{k_{on}}{\rightleftharpoons}} PL \quad (1)$$

$$K_d = \frac{k_{off}}{k_{on}} \quad (2)$$

and to the case where two peptides bind to TnC

$$P + L \underset{k_{on}}{\overset{k_{off}}{\rightleftharpoons}} PL + L \underset{k_{off_2}}{\overset{k_{on_2}}{\rightleftharpoons}} PL_2 \quad (3)$$

where P designates TnC, L the TnI peptide ligand, and PL and PL_2 stand for the protein·peptide and protein·2peptide complexes, respectively. Fitting was performed using a nonlinear least-squares technique (see ref *21* and references therein). For the TnI_{96-139} and TnI_{96-148} titrations the chemical shift changes were not in the intermediate−fast NMR chemical exchange limit required for this approach.

For the longer peptides, spectra taken during the titrations were analyzed using a full line shape analysis (see below) to determine the dissociation rate constant (under an assumption of 1:1 binding). The dissociation constant is a parameter of this fitting process. However, because of the relatively high concentrations used for NMR spectroscopy, the fitting is not sensitive to the value of K_d once the dissociation constant is tighter than approximately 1 μM. This is the case for the TnI_{96-139} and TnI_{96-148} titrations, and thus only an upper limit for the K_d is determined. A lower limit for K_d can be determined from the fitted value of k_{off} and an upper limit for the value of k_{on} ($\leq 1 \times 10^8$ M^{-1} s^{-1}; see refs *63*−*65* and references therein) using eq 2.

Line Shape Analysis. The ^{15}N-labeled TnC was monitored by 2D-^{15}N,^1H-HSQC NMR spectroscopy during each point of the titration, for each of the different TnI peptides. Spectral cross-peaks of backbone amides were then analyzed for changes in chemical shift and line shape during the titrations. Residues from each of the N- and C-terminal domains of troponin-C (Asp^{32} and Lys^{107}, respectively) were chosen that specifically had chemical shift changes only in the proton dimension. The lack of chemical shift changes in the nitrogen dimension allowed for easier cross-peak simulation and cross-peak display. The program Mathematica (*66*) was used as previously described (*21*) to simulate the spectral line shapes of the selected residues during each titration, except that the script file was modified from the previous study to better simulate the effect of dilution on TnC peak intensity.[2] The k_{off} was modified manually in an iterative manner until the best observable fit was obtained. The backbone amide cross-peaks for Glu^{16}, Val^{65}, and Gly^{119} were also checked (data not shown), to ensure that the line width behavior was consistent with other residues.

RESULTS

Two-dimensional ^1H,^{15}N-HSQC NMR spectroscopy was used to elucidate the interaction of three different length TnI peptides with labeled, calcium-saturated chicken skeletal TnC. The three TnI peptides corresponded to regions 96−131, 96−139, and 96−148, respectively. Initially the TnI peptides were unlabeled, while the TnC protein was ^{15}N-labeled. This was done to allow the specific NMR observation of TnC in the complex without interference from TnI resonances. The HSQC NMR spectra display backbone and side chain amide cross-peaks that are sensitive to changes in their local environment and thus allow the monitoring of the titration at the amino acid residue level of resolution. Subsequently, ^{15}N-labeling was incorporated into the TnI_{96-148} peptide, while the TnC was deuterated to minimize signal loss and focus on peptide residues. In the case of the ^{15}N-labeled TnI_{96-148}, 2D ^{15}N edited TOCSY and NOESY NMR spectroscopy was used to identify peptide amino acid spin systems after addition of one equivalent of deuterated TnC. A TnI_{96-139} peptide (^{13}C-TnI_{96-139}) was synthesized incorporating uniformly ^{13}C-labeled leucine (position 102 and 111 at 100% and 50% label, respectively) and ^{13}C-methyl-labeled methionine (positions 121 and 134 at 100% and 50% label, respectively). ^{13}C-HSQC was used to monitor the effect of TnC addition to the ^{13}C-TnI_{96-139} peptide.

Titrations of TnC with TnI_{96-131}, TnI_{96-139}, and TnI_{96-148} are shown in Figure 1 panels A−C, respectively, using contour representations of HSQC spectra. Not all cross-peaks are affected equally, indicating that some TnC residues have a greater change in their local environment than others; however, changes experienced by individual cross-peaks are very similar when comparing the effect of different peptides. The spectral changes induced in the N-domain of intact TnC upon addition of the TnI_{96-131} peptide resemble quite closely the spectra seen for the $TnI_{115-131}$ and TnI_{96-148} peptides when added to the isolated N-terminal domain of troponin-C (*19*, *21*). The largest difference between the three titrations shown in Figure 1 is the change in NMR cross-peak behavior from intermediate−fast exchange with the TnI_{96-131} peptide, to intermediate−slow exchange with the TnI_{96-139} and TnI_{96-148} peptides. In the NMR fast exchange limit a single cross-peak is observed with a chemical shift that is a weighted average of the free and bound chemical shifts. In the slow exchange limit two cross-peaks are observed, one with the chemical shift of the free species and one with the chemical shift of the bound species. In the slow limit the intensity of each peak represents the relative abundance of each species. We do not observe spectra in either the extreme slow or fast exchange limits (see detailed line shape and chemical shift analysis below), but instead see a mixture dependent upon the total chemical shift and respective rates of complex dissociation.

Chemical Shift Analysis and Determination of Dissociation Constants. The observed total chemical shift change (*21*) was used to determine a dissociation constant for the reaction of TnI_{96-131} with TnC. This titration exhibited spectra in the intermediate−fast exchange limit. Chemical shift assignments for TnC were taken from Slupsky et al. (*67*). A total of 85 backbone amide HSQC cross-peaks (out of 162 possible) were followed during each point of the titration (Figure 2) from which $\Delta\delta_{total}$ (*21*) was determined. Figure 2, panels A and B, show the best fit for a 1:1 and 1:2 binding of TnC to TnI_{96-131}, respectively. The 1:1 binding was best fit with a K_d of 32 ± 16 μM, while the 1:2 binding analysis yielded a K_{d1} of 1−50 μM and a K_{d2} of ~2 mM. The binding of two peptides to TnC was considered because a second binding

[2] The new and previous Mathematica scripts used are available upon request from brian.sykes@ualberta.ca or ryan.mckay@ualberta.ca.

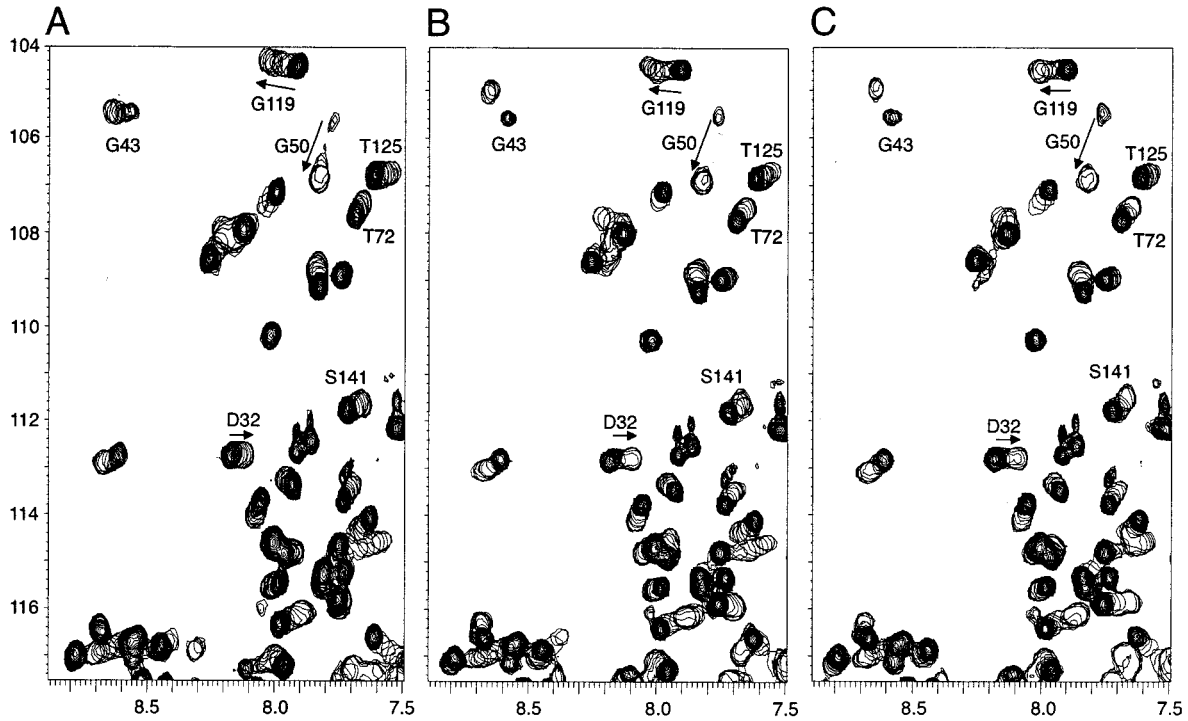

FIGURE 1: Contour plots of an expanded region of the 2D-^{1}H,^{15}N-HSQC NMR spectra taken of ^{15}N-labeled TnC upon titration with unlabeled peptide: (A) TnI_{96-131}, (B) TnI_{96-139}, and (C) TnI_{96-148}, respectively. Panel A shows the addition of 0, 0.2, 0.3, 0.5, 0.6, 0.8, 1.0, 1.1, 1.3, 1.4, and 1.5 molar equiv of TnI_{96-131}, B shows the addition of 0, 0.1, 0.3, 0.4, 0.6, 0.7, 0.9, 1.0, 1.2, 1.3, and 1.5 molar equiv of TnI_{96-139}, and C shows the addition of 0, 0.1, 0.2, 0.3, 0.45, 0.6, 0.7, 0.8, 0.9, 1.1 molar equiv of TnI_{96-148}. Uncomplexed TnC cross-peaks are plotted with more contours while overlaying single contour cross-peaks show the effect of peptide addition. The different effect on cross-peaks experiencing fast-intermediate or slow exchange is very evident in residues such as Gly^{43}, Asp^{32}, and Gly^{50} when comparing the addition of TnI_{96-131} (A) and the two larger peptides (B and C). Residues experience changes of magnitude and direction similar to those of their amide chemical shift in all three titrations. The one letter code is used for marked residues in the figure.

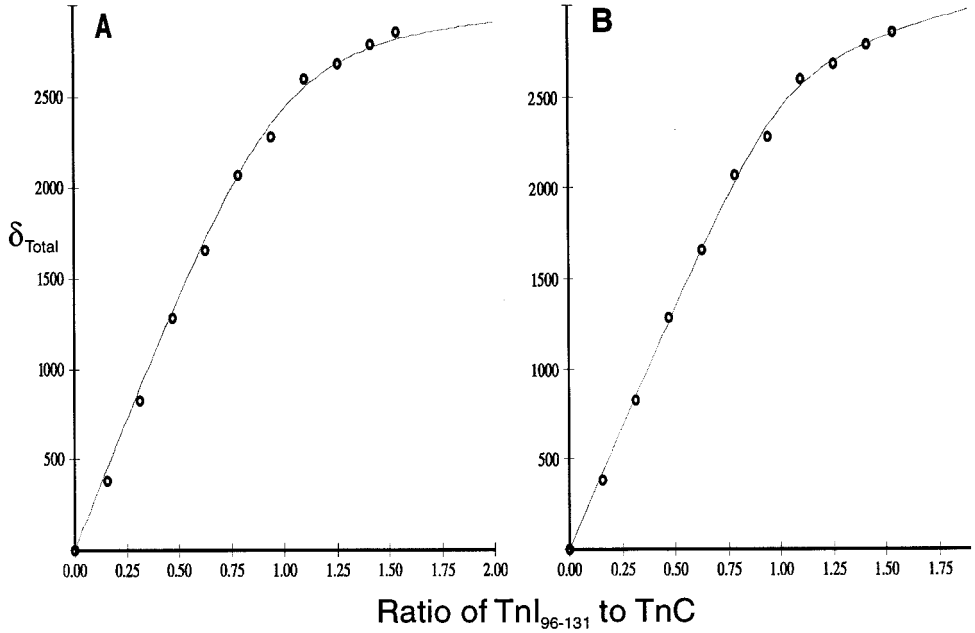

FIGURE 2: Binding curves derived from the 2D-^{1}H,^{15}N-HSQC spectra of labeled TnC upon addition of TnI_{96-131}. The $\Delta\delta_{total}$ for the 85 TnC backbone amide pairs that were monitored throughout the TnI_{96-131} titration as a function of the molar ratio of TnI_{96-131}·TnC with a 1:1 binding curve fit analysis (see text) is shown in panel A, while (B) is the same data fit with a 1:2 binding of TnC to TnI_{96-131}.

event was observed when excess peptide was added (Figure 3). In Figure 3 (especially Panel G) initial peptide binding (i.e., cross-peak broadening) can be seen. Subsequently, coupling of peptide binding and breakup of the TnC dimer results in sharpening of the N-TnC cross-peak line width up to a 1:1 ratio. In the presence of excess TnI peptide, TnC cross-peaks again broaden. This is probably due to competition for both the N- and C-terminal TnC domains by more than one TnI peptide. Since the initial binding event is so much stronger (i.e., $K_{d1} \ll K_{d2}$), the second event can be assumed to be negligible and a value of 32 μM was used during the line shape analyses (see below).

Line Shape Analysis and Determination of Exchange Rates. The dissociation rate constants for all three complexes

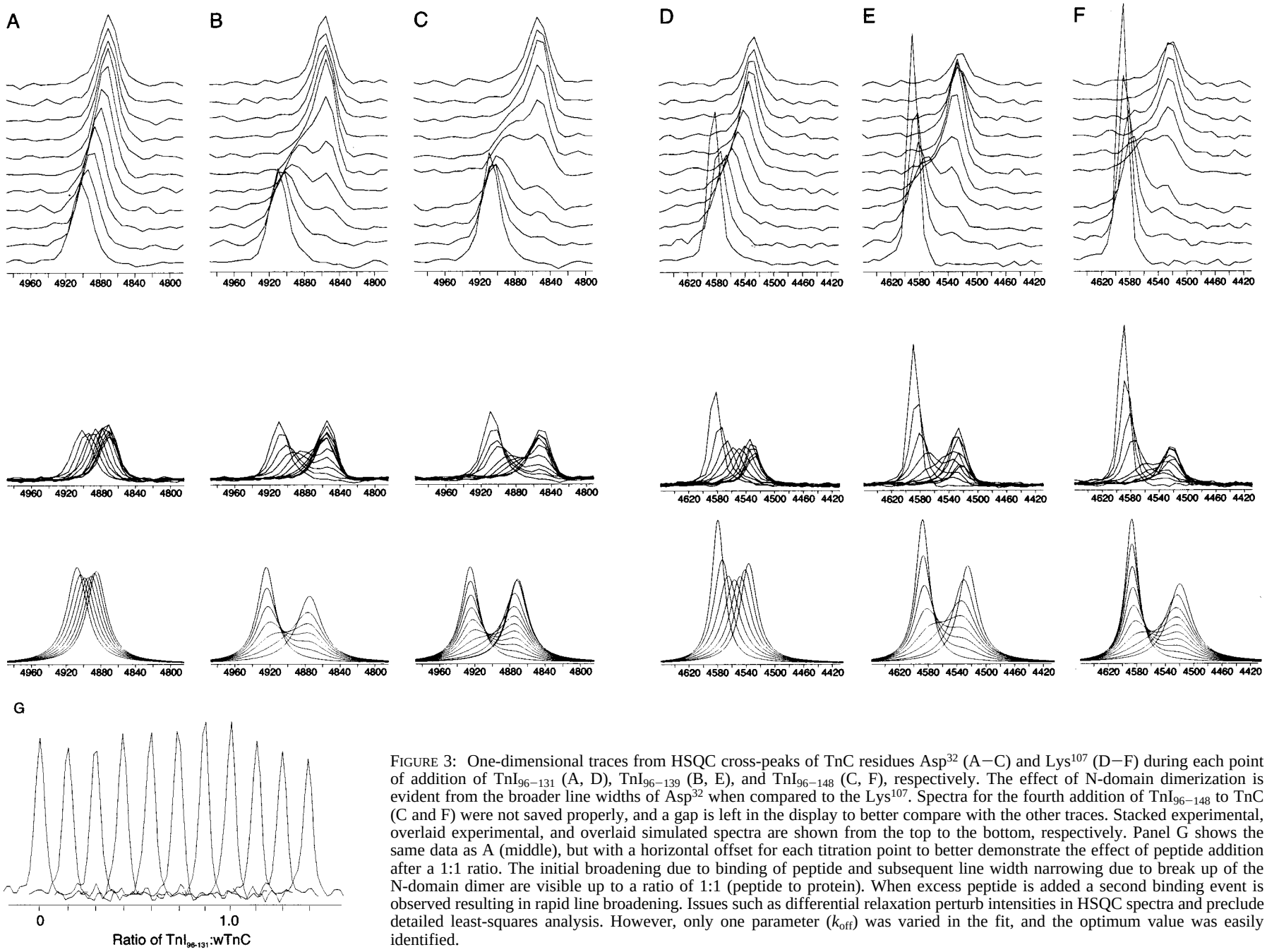

FIGURE 3: One-dimensional traces from HSQC cross-peaks of TnC residues Asp[32] (A−C) and Lys[107] (D−F) during each point of addition of TnI_{96-131} (A, D), TnI_{96-139} (B, E), and TnI_{96-148} (C, F), respectively. The effect of N-domain dimerization is evident from the broader line widths of Asp[32] when compared to the Lys[107]. Spectra for the fourth addition of TnI_{96-148} to TnC (C and F) were not saved properly, and a gap is left in the display to better compare with the other traces. Stacked experimental, overlaid experimental, and overlaid simulated spectra are shown from the top to the bottom, respectively. Panel G shows the same data as A (middle), but with a horizontal offset for each titration point to better demonstrate the effect of peptide addition after a 1:1 ratio. The initial broadening due to binding of peptide and subsequent line width narrowing due to break up of the N-domain dimer are visible up to a ratio of 1:1 (peptide to protein). When excess peptide is added a second binding event is observed resulting in rapid line broadening. Issues such as differential relaxation perturb intensities in HSQC spectra and preclude detailed least-squares analysis. However, only one parameter (k_{off}) was varied in the fit, and the optimum value was easily identified.

Table 1: Kinetics and Energetics of TnI Peptide Binding to TnC

complex	k_{off} (s^{-1})[a] (Asp^{32}, Lys^{107})	K_d (μM)	$\Delta G°_{binding}$ (kcal mol^{-1})[b]	$\Delta G^{‡}_{off}$ (kcal mol^{-1})[c] (Asp^{32}, Lys^{107})
TnC·TnI_{96-131}	400, 400	32 ± 16[d]	-6.2 ± 0.3	14.1, 14.1
TnC·TnI_{96-139}	55, 75	0.5 → 1[e]	−8.7 → −8.3	15.3, 15.1
TnC·TnI_{96-148}	40, 50	0.4 → 1[e]	−8.9 → −8.3	15.5, 15.4

[a] The degree of uncertainty for k_{off} is a factor of 2. [b] Calculated using $\Delta G° = -RT \ln K_d$. Error reported for $\Delta G°$(TnC·TnI_{96-131}) is half the difference in calculated $\Delta G°$ between the upper and lower limit of the reported K_d. [c] Calculated using $\Delta G^{‡}_{off} = -RT \ln(k_{off}h/kT)$. [d] Reported value is for a 1:1 binding analysis. [e] The range for the reported K_d is between the limit of accurate measurement (i.e., 1 μM) and the lower limit based upon an on-rate constant less than or equal to the diffusion limit (i.e., $\sim 1 \times 10^8$ M^{-1} s^{-1}).

were determined from a detailed line shape analysis at each point of the titration, of an amide proton spectral cross-peak corresponding to an amino acid in both the N- and C-terminal domains of TnC. For the TnI_{96-139} and TnI_{96-148} titrations, the K_ds were also estimated from these simulations since chemical shifts could not be used directly. Analysis of cross-peaks at each addition is critical to properly simulate the effect on cross-peak line width. Residues Asp^{32} and Lys^{107} (from the N- and C-terminal domains respectively) were chosen for analysis because they display different degrees of chemical shift changes (e.g., ~30 Hz for Asp^{32}, and ~55 Hz for Lys^{107}) and because both changed primarily in the ^1H dimension. This made simulation of the cross-peaks solely dependent on one nuclei's chemical shift change and display of the cross-peaks far easier (i.e., traces corresponding to a single ^{15}N spectral frequency could be displayed throughout). A comparison of experimentally observed and mathematically simulated one-dimensional traces through the backbone amide cross-peaks of Asp^{32} and Lys^{107}, at each point of all three TnI peptide titrations, is shown in Figure 3, panels A−C and D−F, respectively. The experimental one-dimensional traces (stacked and overlaid) are presented above the simulated spectra. The two residues of TnC monitored during the TnI_{96-131} titration show intermediate−fast exchange, with Lys^{107} displaying more broadening (due to its larger chemical shift change) than Asp^{32}. When the same residues are compared for the TnI_{96-139} and TnI_{96-148} titrations, virtually identical intermediate−slow exchange broadening and chemical shift changes are observed, indicating similar dissociation rate constants for both larger TnI fragments. This indicates that binding of the longer two TnI peptides is much tighter to intact TnC than that of TnI_{96-131}.

The determined off-rate constants, dissociation equilibrium constants, free energy of binding, and free energy of reverse-activation for all three titrations are shown in Table 1. A lower limit for the K_ds for the TnI_{96-139} and TnI_{96-148} titrations were estimated from the determined off-rate constants that best fit the observed spectra and the assumption that k_{on} could be no faster than the lower diffusion rate limit, $\sim 1 \times 10^8$ M^{-1} s^{-1} (*63*−*65*, *68*). The K_d was checked by manually changing the value, reoptimizing k_{off}, and observing if the resulting simulated peaks better matched the experimentally obtained spectra. In all cases the originally determined K_d yielded the best fit.

Backbone amide cross-peak resonance overlap prevented the use of chemical shift mapping (*63*, *69*−*71*) to completely identify the regions of TnC bound by the TnI peptides. This was due to the increased line width and number of cross-peaks from TnC as compared to previous studies using the N-terminal domain of TnC (*19*, *21*). The well-resolved residues did provide enough information to show that when bound the two domains of TnC adopted line widths more representative of a 24 kDa molecule. This conclusion is made from the observed line widths of the N- and C-domains (Table 2) and predicted line widths based on the molecular weight of TnC and TnC complexes (*72*). As expected the N-terminal residues are relatively broad (Figure 3, panels A−C, G) at the beginning of the titration, presumably due to N-terminal dimerization (*73*). The C-terminal peaks lack the initial dimerization and thus only broaden upon peptide addition (Figure 3 panels D−F, and Table 2).

Table 2: NMR Cross-peak Line Widths of TnC N- and C-terminal Domain Residues before and after Titration with TnI Peptides

titration	TnC (Hz) (Asp^{32}, Lys^{107})	complex (Hz) (Asp^{32}, Lys^{107})	complex mass (Da)[a]
TnI_{96-131}	28, 20	25, 25	23416[b]
TnI_{96-139}	24, 23	27, 31	23587
TnI_{96-148}	24, 21	28, 37	24766

titration	TnC (Hz) (Ile^{37}, Ile^{113})	TFE addition (Hz) (Ile^{37}, Ile^{113})
TnC[c]	34, 26	26, 26

[a] The molecular weight of ^{13}C,^{15}N-labeled TnC is 19.2×10^3 g/mol and of ^{15}N,^{13}C(Ala)-labeled TnC is 18.5×10^3 g/mol. [b] TnC used in the TnI_{96-131} titration was labeled with both ^{15}N and ^{13}C, while the TnC in the TnI_{96-139} and TnI_{96-148} samples was only labeled with ^{15}N (and ^{13}C on alanine residues). [c] Results of Slupsky et al. (1995) (*73*) showing disruption of N-domain dimerization upon addition of 13% TFE. Line widths are not directly comparable to the present data because of differences in experimental and processing conditions.

Assignment of TOCSY and NOESY Spectra of ^{15}N-TnI_{96-148}. To define which residues of TnI are interacting with TnC, we studied ^{15}N-labeled TnI_{96-148} both free and when complexed with deuterated TnC. We have observed in the proton spectrum of a shorter TnI peptide (residues 115−131) that the chemical shift dispersion of amide resonances increased when the temperature was lowered from 30 to 5 °C and the pH lowered from 6.85 to 6.35 (data not shown). This indicated that some intrinsic structure may form in the isolated peptide, and this was tested with ^{15}N-labeled TnI_{96-148}. Chemical shift changes in the one-dimensional ^1H and 2D-HSQC spectra were seen in isolated ^{15}N-labeled TnI_{96-148} when the temperature was reduced from 40 to 5 °C, though line broadening severely affected the spectra (data not shown). Decreasing the pH from 6.85 to 6.25 did not significantly increase chemical shift dispersion.

The HSQC spectrum of ^{15}N-labeled TnI_{96-148} changed dramatically upon addition of TnC. Most of the peptide backbone amide resonances broadened and rapidly disappeared (Figure 4). Line broadening is expected when the molecular weight of a species increases. Surprisingly, eleven peptide amide resonances remained sharp, indicating a much smaller change in τ_{rot} (Figure 4, panel B) upon binding of TnC. These cross-peaks also experienced relatively small changes, if any, to their chemical shifts, suggesting little or no change in environment upon protein binding. Two-dimensional versions of 3D-^{15}N-edited TOCSY and ^{15}N-edited NOESY spectra (Figure 5) of the TnI_{96-148} peptide complexed to TnC were taken in an effort to identify those

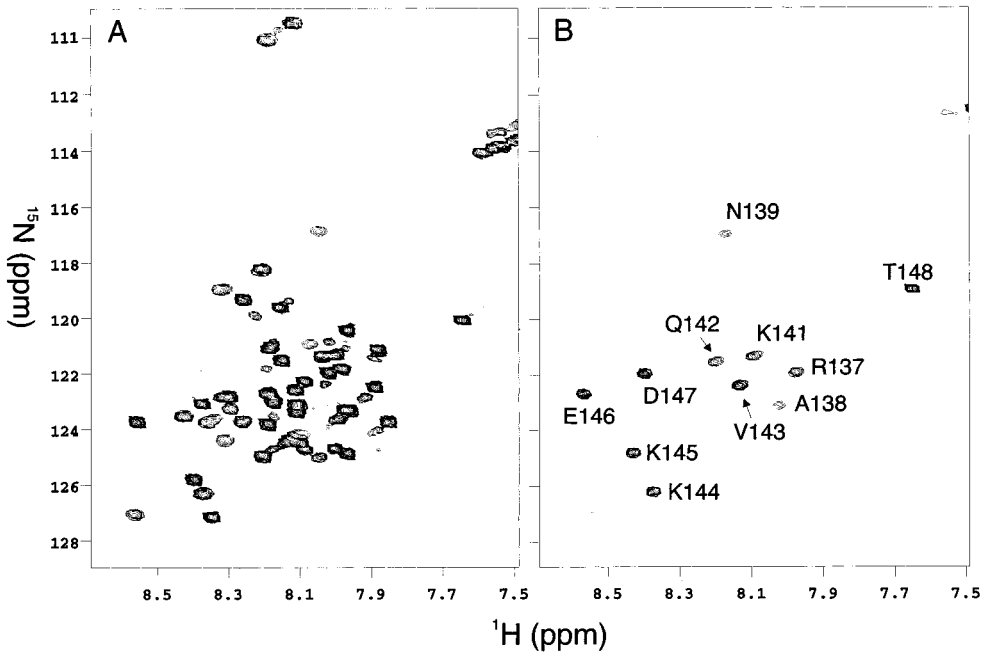

FIGURE 4: Contour plot of 2D-^{1}H,^{15}N-HSQC NMR spectra of ^{15}N-labeled TnI$_{96-148}$ before (A) and after (B) addition of 1 equiv of deuterated TnC. The threshold and vertical scale are identical between the two plots to show the change in line widths of TnI residues upon addition of protein. The eleven cross-peaks remaining in the spectra appear to be unperturbed by TnC binding and were assigned via TOCSY and NOESY NMR experiments. The one letter code is used to label assigned TnI residues in panel B. Broad poorly resolved resonances are observed at lower contour levels for panel B.

peptide backbone amide residues relatively unperturbed by TnC binding. The NMR spin systems of the unperturbed residues from TnI$_{96-148}$ were identified from the TOCSY (Figure 5, panel A) experiments, while the sequential order was established from the NOESY information (Figure 5, panel B). Spin system information is degenerate for some amino acids (i.e., Asn and Asp have very similar TOCSY spectra), and therefore the known peptide amino acid sequence was used to identify degenerate residues that had NOE contacts to distinct amino acids (e.g., Glu^{146} had short-range NOEs to Lys^{145} but not Lys^{144}, thus making the two degenerate Lysine residues assignable). The eleven unperturbed residues have been assigned on the basis of their individual spin system and interresidue NOEs to the last eleven residues of the C-terminal end of the TnI$_{96-148}$ peptide (Figure 6). An additional unperturbed amide resonance was tentatively assigned to Arg^{137}, but the possibility of this cross-peak belonging to Asn^{96} (i.e., the N-terminal residue) could not be eliminated. The observed chemical shifts for the assigned TnI hydrogen atoms correspond to the random coil chemical shifts (*56*, *74*, *75*), indicating no defined secondary structure. Therefore the last eleven residues appear to be rotating freely (i.e., relatively short τ_c) and in a random coil in the presence or absence of TnC.

Monitoring of ^{13}C-TnI$_{96-139}$ upon Addition of TnC. The ^{13}C-TnI$_{96-139}$ peptide (Figure 6) was complexed to TnC, and Figure 7 shows contour plots of the coupled ^{13}C-HSQC spectra of the ^{13}C-TnI$_{96-139}$ methionine and leucine methyl groups (panels A and C), respectively. In these plots, cross-peaks are split along the ^{1}H NMR axis by the $^{1}J_{CH}$ coupling constant values of ~138 Hz (~0.28 ppm) and 123 Hz for the Met and Leu residues, respectively. The two methionines (panel A) of the free peptide are equivalent in ^{13}C NMR resonance frequencies but separated by 5 Hz in the ^{1}H NMR dimension. The 100% and 50% labeling for Met^{121} and Met^{134}, respectively, can be observed in the 1D trace taken through the cross-peaks at the position of the dotted line and displayed at the bottom of panel A. The ^{1}H,^{13}C-HSQC spectra of each of the two methyl groups (also split by $^{1}J_{CH}$) from each of the two leucine residues in the free and bound ^{13}C-TnI$_{96-139}$ peptides are shown in panels C and D, respectively. TnI leucine residues102 and 111 were 100% and 50% labeled with ^{13}C, respectively, and the relative intensities are evident in both the free and bound spectra (Figure 7, panels C and D, respectively). Most striking are the different behaviors for the spectra of Leu^{102} and Leu^{111} (panel D) versus Met^{121} and Met^{134} (panel B) in the bound complex. For each methyl group from Leu^{102} and Leu^{111}, there is only a single, coupled cross-peak, albeit shifted and broadened due to the binding of TnC. However, residues Met^{121} and Met^{134} (Figure 7, panel B) show at least 4 pairs of chemically shifted cross-peaks at ~17.5 ppm (^{13}C NMR axis) with much broader line widths than that of the free peptide. Also there is another sharp, but low-intensity coupled cross-peak at ~17.05 ppm (^{13}C) which corresponds to the proton chemical shift of Met^{134}. This implies that several different states exist.

DISCUSSION

The off-rate and dissociation constants have been determined for three TnI peptides interacting with TnC. On the basis of these dissociation constants and off-rates, we have calculated the free energy of binding and estimated the activation energy barriers for both the forward and reverse reactions. We have also identified eleven C-terminal residues in TnI$_{96-148}$ that do not interact with TnC. The results indicate that residues 97−136 (and possibly 96 or 137) are directly interacting with TnC. Residues 138−148 (and possibly 137 or 96) do not appear to interact with TnC, nor does the presence or absence of these extra TnI residues significantly

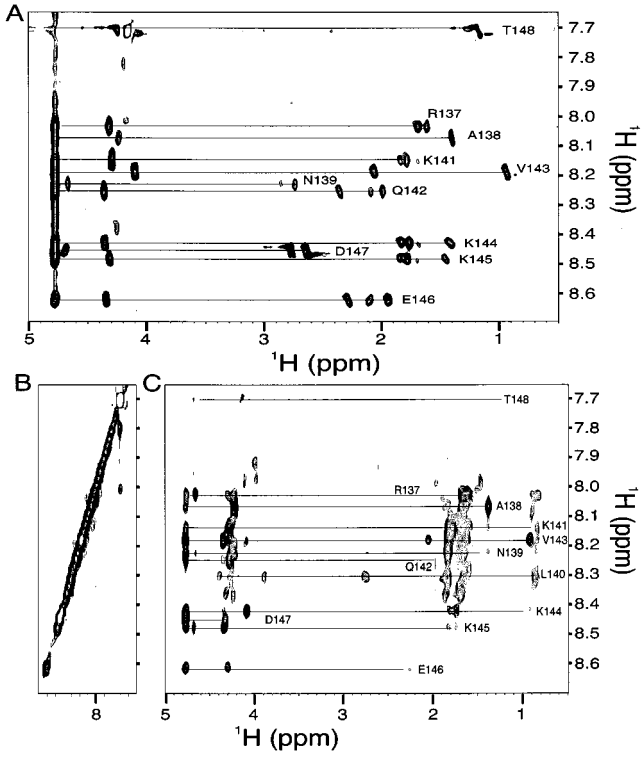

FIGURE 5: Expanded contour plots of two-dimensional, ^{15}N-edited (A) TOCSY and (B, C) NOESY spectra of ^{15}N-labeled TnI_{96-148} complexed to deuterated TnC. Panels A and C show the aliphatic region of the TOCSY and NOESY spectra, respectively, while B shows the NOESY amide region. The lack of amide to amide cross-peaks (B) made sequential assignment dependent on accurate spin-system identification and aliphatic NOEs. The aliphatic NOEs also provided necessary information to assign degenerate spin systems such as Asn^{139}/Asp^{147} and Glu^{146}/Gln^{142}. Important NOESY contacts include the NOE of Lys^{141} to the methyl of Leu^{140}, and the similar contact of Lys^{144} to the methyl of Val^{143}. Thr^{148} could be assigned on its unusually intense cross-peaks, characteristic of a flexible C-terminal residue. Interestingly Leu^{140} only appears in the NOESY spectra. A total of 10 unambiguous aliphatic NOEs allowed the deduction of the region of the TnI_{96-148} peptide not affected by TnC addition.

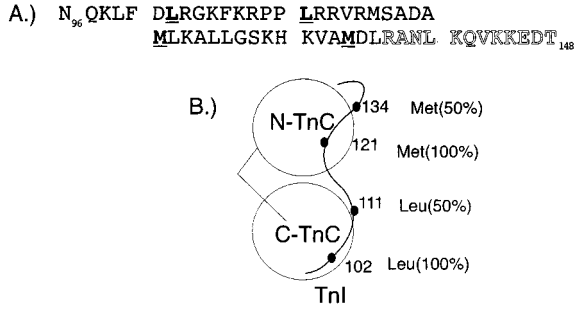

FIGURE 6: (A) Sequence of TnI residues 96−148 showing the eleven C-terminal residues (outline) not perturbed by TnC binding. Arg^{137} is also shown outlined to indicate possible inclusion in this assignment (see text). Residues shown underlined and boldfaced indicate the positions of two leucines (residues 102 and 111) and methionines (residues 121 and 134) labeled with ^{13}C in the synthetic ^{13}C-TnI_{96-139} peptide. (B) Cartoon representation of the interaction of TnC with TnI. The ^{13}C-labeled amino acids are shown with their relative abundance.

reduce the affinity of complex formation. Removing residues 132−139 reduces the affinity of TnI for TnC, increases the dissociation rate constant for the complex, and appears to reduce the ability of TnI to restrict the two domains of TnC into a more constrained conformation. Partial dimerization

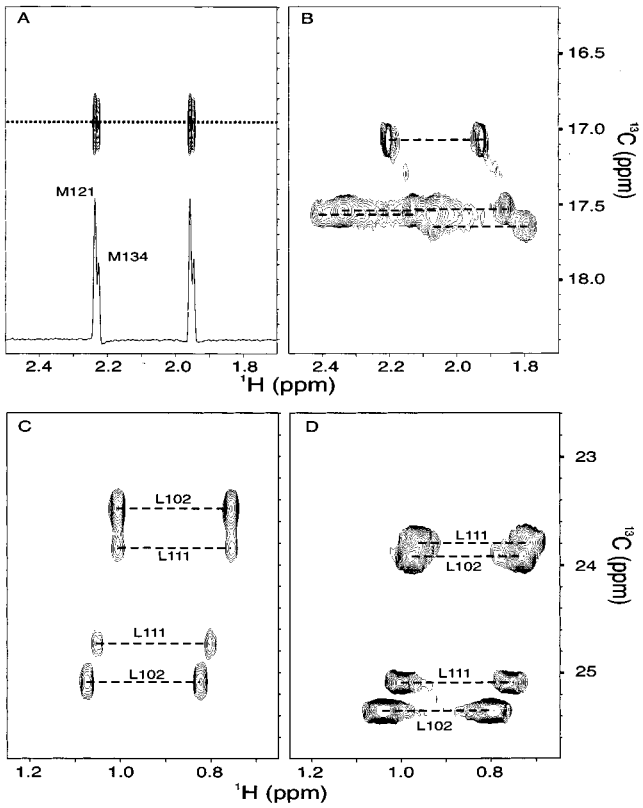

FIGURE 7: Contour plots of an expanded region of carbon-coupled 2D-^{1}H,^{13}C-HSQC NMR spectra taken of [U-^{13}C] (100% labeled) Leu^{102}, (50%) Leu^{111}, [$^{13}CH_3$] (100%) Met^{121}, and (50%) Met^{134}-TnI_{96-139} free and bound to TnC. The spectral region for the methionine resonances is shown in panels A and B for free and bound TnI_{96-139} peptide, respectively. The dotted line in A shows the position from which the 1D trace of the ^{13}C-HSQC cross-peak (A, bottom) was taken to display the pairs of coupled cross-peaks with the relative abundance. Panels C and D show the NMR spectral region for the leucine methyl groups of TnI_{96-139} free and bound to TnC, respectively. Carbon decoupling in the directly detected dimension was not performed to allow extended acquisition and therefore resolution of the closely degenerate methionine methyl resonances. Dashed lines show coupled sets of cross-peaks. One-letter codes are used for the residues in the figure.

of TnC via the N-domain (*73*) of TnC is disrupted upon peptide addition as is evident by slight narrowing of N-terminal TnC residues (Figure 3, panel G, and Table 2).

Energetics. Previous studies have shown that several regions of TnI have affinity for either, or both, domains of TnC. TnI_{96-116} have been shown to bind ($K_d \approx 3-0.5$ μM) to the C-terminal domain of TnC (refs *47*, *76*, and references therein), while the 115−131 region of TnI has been shown to bind ($K_d \approx 20$ μM) to N-TnC (*19*, *21*, *46*, *47*). If we consider that the TnI_{96-148} peptide binds simultaneously to both domains of TnC, and that the binding free energy is the sum of the individual binding components (i.e., the observed K_d is the product of the individual K_ds for both domains, respectively), then one would expect to see a dissociation constant for TnI_{96-148}·TnC in the 1−100 pM range. This is not the case as we observe a K_d of ∼500 nM. Further, the combination of an off-rate constant in the range 40−75 s^{-1} and a dissociation constant in the picomolar range would require a k_{on} of 1×10^{13} M^{-1} s^{-1}, approximately 5 orders of magnitude faster than the diffusion limit (*63*). The weaker observed binding (i.e., ∼12−24 kcal mol^{-1}) may be a result of several factors: (1) the entropic cost of restricting

the two domains of TnC; (2) strain and/or negative interactions in the TnI "linker" region; (3) shifting of either region of TnI in relation to TnC (e.g., the 115−131 region of TnI_{96-139} and TnI_{96-148} may be binding in a slightly different position relative to TnC than compared to $TnI_{115-131}$ bound to the isolated N-TnC); and (4) the lack of C-terminal residues may disrupt secondary structure of binding residues because of "fraying" (*77*) or disordering. This end "fraying" may also explain the suspected Met^{134} "free" species observed with ^{13}C-TnI_{96-139}·TnC complex. Additionally, it is possible that the observed TnI peptide off-rates are for each individual domain of TnC and not the whole molecule. This would require identical and noncooperative binding of the two regions of TnI to both domains of TnC which has not been reported. In general, these kinds of concerns may be relevant when using peptides.

In previous NMR studies, no significant difference in binding strength was observed when comparing the interaction of $TnI_{115-131}$ ($K_d = 24 \pm 4$ μM) and TnI_{96-148} (K_d = 1−40 μM) with the N-domain of TnC (*19*, *21*), whereas we see interactions of TnI residues 131−136 with TnC. As discussed above, if the regions of TnI that interact with TnC shift when comparing binding to whole TnC and the isolated N-domain, then the remaining residues (i.e., 131−136) could become more important. These residues may also interact with an area of TnC other than the calcium-regulated hydrophobic pocket. There is some supportive evidence for this because intermolecular NOE contacts were observed in the TnI_{96-148}·N-TnC study on the side of TnC opposite that of the hydrophobic pocket (termed the backside) (*19*, *37*, *78*). Recently the structure of the cardiac equivalent of $TnI_{115-131}$ bound to the N-domain of cardiac TnC has been solved, and residues equivalent to 115−127 of skeletal TnI have been shown to bind in the hydrophobic pocket of cardiac N-TnC (*79*, *80*). This information supports the idea that residues 131−136 bind to TnC residues outside the hydrophobic pocket, or may suggest that different TnI residues bind to TnC in the cardiac and skeletal systems. The 127−131 region of TnI is 100% identical over all compared species (fast skeletal chicken, quail, rabbit, human, mouse, slow skeletal mouse, rabbit, human, and rat), suggesting that the region is more than merely a structural loop (see ref *47* for a more detailed sequence comparison). This does not necessarily require that 127−131 is actively involved in specific TnC binding since this region may be important in the interaction with actin, TnC, or both.

Mechanism and Models. There is ample evidence that TnC and TnI interact in an antiparallel orientation. Specifically, recent results show that TnI regions 115−131 and 96−115 bind to the N- and C-terminal domains of TnC, respectively (see refs *2*, *19*, *21*, *76*, and references therein). The present results indicate that leucines 102 and 111 in the N-terminal portion of ^{13}C-TnI_{96-139} bind in a single orientation while complexed to TnC. However, methionines 121 and 134 in the C-terminal portion of the ^{13}C-labeled peptide bind in multiple conformations. The spectra show at least four pairs of broad cross-peaks shifted from the free peptide resonance frequencies (Figure 7B), suggesting at least two bound environments for each of the two methionine residues. Interestingly, the coupled cross-peak resonating at a ^{13}C chemical shift of 17.1 ppm has the same ^{1}H and ^{13}C chemical shift (within digital resolution) of free Met^{134} but is slightly broadened. This leads to the possibility that Met^{134} may also exist in a random coil and relatively free conformation while the N-terminal portion of the TnI peptide (containing Leu^{102} and Leu^{111}) is bound to the C-domain of TnC. The number of bound peaks suggests that there may be up to three conformations, described by two different binding models for Met^{121}/Met^{134} even when the N-terminal region of the TnI peptide is "tethered" to the C-domain of TnC. Two of the simplest schemes are shown (Scheme 1).

Scheme 1

$$\begin{array}{ccc} Peptide \rightleftarrows Complex & & \\ \uparrow\downarrow & \text{or} & Peptide \rightleftarrows Complex \rightleftarrows Complex^* \\ Complex^* & & \end{array}$$

In Scheme 1 (left), Complex and Complex* represent TnI_{96-139} tethered to C-TnC via the 96−115 TnI region, and subsequently binding in two distinct N-TnC sites. In Scheme 1 (right), Complex and Complex* represent two kinetically relevant species, both of which are tethered to C-TnC as in Scheme 1 (left) but with both Complex and Complex* (e.g., representing different TnI peptide conformations) binding to a single site in N-TnC. This is the first time that peptide promiscuity has been observed for TnI binding to TnC. It is attractive to speculate that the three states are relevant to the three states shown to exist for the regulation of the thin filament (ref *81* and references therein). In this situation complex and complex* would be the TnC·TnI states corresponding to the closed and open states of the thin filament.

Previous binding studies have indicated a possible 1:2 binding stoichiometry of TnI peptides to TnC attributed to affinities of the TnI peptides for the N- and C-terminal domains of TnC, respectively (*47*), but was ruled out here because the TnC was present in equimolar concentrations to TnI and only single bound cross-peaks were observed for the leucine TnI resonances.

There are presently two models regarding the interaction of TnC and TnI. The first model suggested separately by Olah et al. (*39*) and Ngai et al. (*50*) suggests that a "switching mechanism" may exist in which TnI residues ∼115−131 bind to the N-domain of TnC in a calcium-dependent fashion, and that the C-domain is bound alternately by residues 96−115 and 1−40 of TnI (also known as Rp40) in the calcium-saturated and apo states, respectively. This model has the advantage that competition between residues 1−40 and 96−115 in TnI might reduce the binding of TnI to calcium-saturated TnC from the reported K_d 0.2−1.7 nM (*82*, *83*) to one more kinetically understandable in regard to observed rates of muscle regulation. The second model suggested by Vassylyev et al. and supported by others has the 1−40 region of TnI bound to the C-domain of TnC regardless of the presence or absence of calcium (*2*, *23*). The Vassylyev model also suggests that the inhibitory region of TnI adopts the NMR structure of the TnIp peptide bound to the C-domain of TnC reported by Campbell et al. (*84*), but instead of binding in the hydrophobic pocket of C-TnC makes few contacts to TnC in the presence or absence of calcium. The second model has been examined by two other groups in regard to TnT interactions (*5*) and resonance energy transfer studies (*31*). At present both models appear to be equally supported though neither model involves interactions of N-TnC with regions 131−136 of TnI. Our findings here

suggest that TnI residues 97−136 (and 96 or 137) bind to both domains of TnC yet do not determine where interaction occurs in the C-domain of TnC.

In this study we have determined the dissociation and off-rate constants of three TnI peptides with intact TnC in the calcium-saturated state, and we have examined the NMR-labeled ^{15}N-TnI$_{96-148}$ and ^{13}C-TnI$_{96-139}$ peptides when in complex with calcium-saturated TnC. Our primary conclusion from this study is that TnI residues 97−136 (and 96 or 137) bind to whole TnC, and that residues ∼138−148 do not interact with TnC. The residues reported here that do not interact with TnC were found by Tripet et al. to be important for binding to actin and for proper regulation of contraction. Additionally residues Leu^{102} and Leu^{111} show single bound conformations to TnC while Met^{121} and Met^{134} show multiple bound species. We would like to suggest that TnI residues 115−136 bind to the calcium-saturated N-domain of TnC (in at least two conformations), with residues 131−136 possibly making "backside" contacts with N-TnC, and that residues ∼97−115 bind to C-TnC.

ACKNOWLEDGMENT

Thanks to Les Hicks and the Cyril Kay Lab for advice and use of their HPLC equipment and lab space. We thank PENCE for use of the 600 MHz NMR spectrometer, and Gerry McQuaid and Bruce Lix for the upkeep of NMR instruments. Thanks to Paul Semchuck for peptide synthesis and to Lewis E. Kay (University of Toronto) for NMR pulse sequences. Special thanks to Leo Spyracopoulos, Monica Li, and Linda Saltibus for support, help, and advice during this work, and to Joel Dacks and Peter Bayley for helpful discussions regarding sequence conservation and peptide-binding energetics and kinetics, respectively.

REFERENCES

1. Tobacman, L. S. (1996) *Annu. Rev. Physiol. 58*, 447−481.
2. Farah, C. S., and Reinach, F. C. (1995) *FASEB J. 9*, 755−767.
3. Potter, J. D., and Johnson, J. D. (1982) in *Calcium and Cell Function* (Cheung, W. Y., Ed.) Vol. 2, pp 145−169, Academic Press, Inc, New York.
4. Leavis, P. C., and Gergely, J. (1984) *CRC Crit. Rev. Biochem. 16*, 235−305.
5. Malnic, B., Farah, C. S., and Reinach, F. C. (1998) *J. Biol. Chem. 273*, 10594−10601.
6. Head, J. F., and Perry, S. V. (1974) *Biochem. J. 137*, 145−154.
7. Syska, H., Wilkinson, J. M., Grand, R. J. A., and Perry, S. V. (1976) *Biochem. J. 153*, 375−387.
8. Li, M. X., Gagné, S. M., Tsuda, S., Kay, C. M., Smillie, L. B., and Sykes, B. D. (1995) *Biochemistry 34*, 8330−8340.
9. Herzberg, O., and James, M. N. G. (1988) *J. Mol. Biol. 203*, 761−779.
10. Satyshur, K. A., Rao, S. T., Pyzalska, D., Drendal, W., Greaser, M., and Sundaralingam, M. (1988) *J. Biol. Chem. 263*, 1628−1647.
11. Rao, S. T., Satyshur, K. A., Greaser, M. L., and Sundaralingam, M. (1996) *Acta Crystallogr., Sect. D 52*, 916−922.
12. Strynadka, N. C. J., Cherney, M., Sielecki, A. R., Li, M. X., Smillie, L. B., and James, M. N. G. (1997) *J. Mol. Biol. 273*, 238−255.
13. Houdusse, A., Love, M. L., Dominguez, R., Grabarek, Z., and Cohen, C. (1997) *Structure 5*, 1695−1711.
14. Gagné, S. M., Tsuda, S., Li, M. X., Smillie, L. B., and Sykes, B. D. (1995) *Nat. Struct. Biol. 2*, 784−789.
15. Gagné, S. M., Li, M. X., and Sykes, B. D. (1997) *Biochemistry 36*, 4386−4392.
16. Slupsky, C. M., and Sykes, B. D. (1995) *Biochemistry 34*, 15953−15964.
17. Spyracopoulos, L., Li, M. X., Sia, S. K., Gagné, S. M., Chandra, M., Solaro, R. J., and Sykes, B. D. (1997) *Biochemistry 36*, 12138−12146.
18. Sia, S. K., Li, M. X., Spyracopoulos, L., Gagné, S. M., Liu, W., Putkey, J. A., and Sykes, B. D. (1997) *J. Biol. Chem. 272*, 18216−18221.
19. McKay, R. T., Pearlstone, J. R., Corson, D. C., Gagné, S. M., Smillie, L. B., and Sykes, B. D. (1998) *Biochemistry 37*, 12419−12430.
20. Gagné, S. M., Li, M. X., McKay, R. T., and Sykes, B. D. (1998) *Biochem. Cell Biol. 76*, 301−312.
21. McKay, R. T., Tripet, B. P., Hodges, R. S., and Sykes, B. D. (1997) *J. Biol. Chem. 272*, 28494−28500.
22. Vassylyev, D. G., Takeda, S., Wakatsuki, S., Maeda, K., and Maeda, Y. (1998) *Biophys. J. 74*, A53.
23. Vassylyev, D. G., Takeda, S., Wakatsuki, S., Maeda, K., and Maeda, Y. (1998) *Proc. Natl. Acad. Sci. U.S.A. 95*, 4847−4852.
24. Nelson, M. R., and Chazin, W. J. (1998) *Protein Sci. 7*, 270−282.
25. Ikura, M., Clore, G. M., Gronenborn, A. M., Zhu, G., Klee, C. B., and Bax, A. (1992) *Science 256*, 632−638.
26. Meador, W. E., Means, A. R., and Quiocho, F. A. (1992) *Science 257*, 1251−1255.
27. Meador, W. E., Means, A. R., and Quiocho, F. A. (1993) *Science 262*, 1718−1721.
28. Rayment, I., Rypniewski, W. R., Schmidt-Base, K., Smith, R., Tomchick, D. R., Benning, M. M., Winkelmann, D. A., Wesenberg, G., and Holden, H. M. (1993) *Science 261*, 50−58.
29. Houdusse, A., and Cohen, C. (1995) *Proc. Natl. Acad. Sci. U.S.A. 92*, 10644−10647.
30. Olah, G. A., and Trewhella, J. (1994) *Biochemistry 33*, 12800−12806.
31. Luo, Y., Wu, J.-L., Gergely, J., and Tao, T. (1997) *Biochemistry 36*, 11027−11035.
32. Tripet, B. P., Van Eyk, J. E., and Hodges, R. S. (1997) *J. Mol. Biol. 271*, 728−750.
33. Tao, T., Scheiner, C. J., and Lamkin, M. (1986) *Biochemistry 25*, 7633−7639.
34. Leszyk, J., Grabarek, Z., Gergely, J., and Collins, J. H. (1990) *Biochemistry 29*, 299−304.
35. Ngai, S.-M., Sönnichsen, F. D., and Hodges, R. S. (1994) *J. Biol. Chem. 269*, 2165−2172.
36. Kobayashi, T., Grabarek, Z., Gergely, J., and Collins, J. H. (1995) *Biochemistry 34*, 10946−10952.
37. Jha, P. K., Mao, C., and Sarkar, S. (1996) *Biochemistry 35*, 11026−11035.
38. Kobayashi, T., Leavis, P. C., and Collins, J. H. (1996) *Biochim. Biophys. Acta 1294*, 25−30.
39. Olah, G. A., Rokop, S. E., Wang, C.-L. A., Blechner, S. L., and Trewhella, J. (1994) *Biochemistry 33*, 8233−8239.
40. Stone, D. B., Timmins, P. A., Schneider, D. K., Krylova, I., Ramos, C. H. I., Reinach, F. C., and Mendelson, R. A. (1998) *J. Mol. Biol. 281*, 689−704.
41. Farah, C. S., Miyamoto, C. A., Ramos, C. H. I., da Silva, A. C. R., Quaggio, R. B., Fujimori, K., Smillie, L. B., and Reinach, F. C. (1994) *J. Biol. Chem. 269*, 5230−5240.
42. Van Eyk, J. E., and Hodges, R. S. (1988) *J. Biol. Chem. 263*, 1726−1732.
43. Van Eyk, J. E., Thomas, L. T., Tripet, B. P., Wiesner, R. J., Pearlstone, J. R., Farah, C. S., Reinach, F. C., and Hodges, R. S. (1997) *J. Biol. Chem. 272*, 10529−10537.
44. Leavis, P. C., Rosenfeld, S. S., and Gergely, J. (1978) *J. Biol. Chem. 253*, 5452−5459.

45. Takeda, S., Kobayashi, T., Taniguchi, H., Hayashi, H., and Maéda, Y. (1997) *Eur. J. Biochem. 246*, 611−617.
46. Pearlstone, J. R., and Smillie, L. B. (1995) *Biochemistry 34*, 6932−6940.
47. Pearlstone, J. R., Sykes, B. D., and Smillie, L. B. (1997) *Biochemistry 36*, 7601−7606.
48. Campbell, A. P., Cachia, P. J., and Sykes, B. D. (1991) *Biochem. Cell Biol. 69*, 674−681.
49. Ngai, S.-M., and Hodges, R. S. (1992) *J. Biol. Chem. 267*, 15715−15720.
50. Ngai, S. M. (1994) *Synthetic peptide studies on troponin C-troponin I interaction*, Ph.D. Thesis, University of Alberta. *94FD NGA*, p 156.
51. Talbot, J. A., and Hodges, R. S. (1979) *J. Biol. Chem. 254*, 3720−3723.
52. Talbot, J. A., and Hodges, R. S. (1981) *J. Biol. Chem. 256*, 2798−2802.
53. Gagné, S. M., Tsuda, S., Li, M. X., Chandra, M., Smillie, L. B., and Sykes, B. D. (1994) *Protein Sci. 3*, 1961−1974.
54. Studier, F. W., Rosenberg, A. H., Dunn, J. J., and Dubendorff, J. W. (1990) *Methods Enzymol. 185*, 60−89.
55. Sambrook, J., Fritsh, E. F., and Maniatis, T. (1989) *Molecular Cloning: A Laboratory Manual*, 2nd ed.; Cold Spring Harbor Laboratory Press, New York.
56. Wishart, D. S., Bigam, C. G., Yao, J., Abildgaard, F., Dyson, H. J., Oldfield, E., Markley, J. L., and Sykes, B. D. (1995) *J. Biomol. NMR 6*, 135−140.
57. Muhandiram, D. R., and Kay, L. E. (1994) *J. Magn. Reson. B103*, 203−216.
58. Kay, L. E., Keifer, P., and Saarinen, T. (1992) *J. Am. Chem. Soc. 114*, 10663−10665.
59. Zhang, O., Kay, L. E., Olivier, J. P., and Forman-Kay, J. D. (1994) *J. Biomol. NMR 4*, 845−858.
60. Delaglio, F., Grzesiek, S., Vuister, G. W., Zhu, G., Pfeifer, J., and Bax, A. (1995) *J. Biomol. NMR 6*, 277−293.
61. Slupsky, C. M. (1995) *The NMR Solution Structure of Calcium-Saturated Skeletal Muscle Troponin C.*, Ph.D. Thesis, University of Alberta, p 352.
62. Wüthrich, K. (1986) *NMR of proteins and nucleic acids*, John Wiley & Sons, New York.
63. Kilby, P. M., Van Eldik, L. J., and Roberts, G. C. K. (1997) *Protein Sci. 6*, 2494−2503.
64. Bayley, P. M., Findlay, W. A., and Martin, S. R. (1996) *Protein Sci. 5*, 1215−1228.
65. Torok, K., Cowley, D. J., Brandmeier, B. D., Howell, S., Aitken, A., and Trentham, D. R. (1998) *Biochemistry 37*, 6188−6198.
66. Wolfram, S. (1996) *The Mathematica Book*, 3rd ed.; (Walsh, J., Beck, G., and Grohens, J., Eds.) Wolfram Media/Cambridge University Press, Cambridge, U.K.
67. Slupsky, C. M., Reinach, F. C., Smillie, L. B., and Sykes, B. D. (1995) *Protein Sci. 4*, 1279−1290.
68. Brown, S. E., Martin, S. R., and Bayley, P. M. (1997) *J. Biol. Chem. 272*, 3389−3397.
69. Lee, A. L., Volkman, B. F., Robertson, S. A., Rudner, D. Z., Barbash, D. A., Cline, T. W., Kanaar, R., Rio, D. C., and Wemmer, D. E. (1997) *Biochemistry 36*, 14306−14317.
70. Rajagopal, P., Waygood, E. B., Reizer, J., Saier, M. H. J., and Klevit, R. E. (1997) *Protein Sci. 6*, 2624−2627.
71. Shuker, S. B., Hajduk, P. J., Meadows, R. P., and Fesik, S. W. (1996) *Science 274*, 1531−1534.
72. Li, M. X., Gagné, S. M., Spyracopoulos, L., Kloks, C. P. A. M., Audette, G., Chandra, M., Solaro, R. J., Smillie, L. B., and Sykes, B. D. (1997) *Biochemistry 36*, 12519−12525.
73. Slupsky, C. M., Kay, C. M., Reinach, F. C., Smillie, L. B., and Sykes, B. D. (1995) *Biochemistry 34*, 7365−7375.
74. Wishart, D. S., and Sykes, B. D. (1994) *Methods Enzymol. 239*, 363−392.
75. Wishart, D. S., Sykes, B. D., and Richards, F. M. (1991) *J. Mol. Biol. 222*, 311−333.
76. Campbell, A. P. (1991) *NMR Studies of the Interactions Between Proteins in the Thin Filament of Muscle*, Ph.D. Thesis, University of Alberta. p 424.
77. Ehrhardt, M. R., Urbauer, J. L., and Wand, A. J. (1995) *Biochemistry 34*, 2731−2738.
78. McKay, R. T. (1999) *Defining the Interactions of Troponin-C with Troponin-I by Nuclear Magnetic Resonance Spectroscopy*, Ph.D. Thesis, University of Alberta (manuscript in preparation).
79. Li, M. X., Spyracopoulos, L., and Sykes, B. D. (1998) *Biophys. J. 74*, A51.
80. Li, M. X., Spyracopoulos, L., and Sykes, B. D. (1999) *Biochemistry* (in press).
81. Schaertl, S., Lehrer, S. S., and Geeves, M. A. (1995) *Biochemistry 34*, 15890−15894.
82. Wang, C. K., and Cheung, H. C. (1985) *Biophys. J. 48*, 727−739.
83. Ingraham, R. H., and Swenson, C. A. (1984) *J. Biol. Chem. 259*, 9544−9548.
84. Campbell, A. P., and Sykes, B. D. (1991) *J. Mol. Biol. 222*, 405−421.

BI9829736